CrystEngComm

PAPER

Fabrication of self-standing films consisting of enamel-like oriented nanorods using artificial peptide

Kazuki Aita,[a] Yuya Oaki,[a] Chikara Ohtsuki[b] and Hiroaki Imai*[a]

We achieved the fabrication of enamel-like films consisting of *c*-axis-oriented hydroxyapatite (HA) nano-rods by a two-step controlled crystal growth method with the monolayer of a specific artificial peptide binding to the *c* face of HA. Self-standing films were formed under the monolayer at the air–water interface in an aqueous solution system that was based on a simulated body fluid. The presence of fluoride ions pro-moted the arrangement of apatite microrods in the *c* direction through geometric selection. The subse-quent growth with aspartic acid produced the enamel-like structure consisting of *c*-axis-oriented nanorods on the basal microrods. Therefore, the controlled crystal growth using the aqueous system including the specific artificial peptide, fluoride ion, and aspartic acid is regarded as a novel fabrication route for well-organized architectures.

Introduction

Hydroxyapatite (Ca$_{10}$(PO$_4$)$_6$(OH)$_2$, HA) is the main mineral component of the hard tissues of mammals. Slender and long HA nanocrystals are assembled with collagen fibers in their natural structures. The dental enamel surface, the outermost layer of teeth, is covered with well-organized rod-like prisms composed of highly oriented bundles parallel to the *c* axis of HA crystals.[1] HA structures having a specific *c*-axis orientation are also observed in various parts of bones.[2] The proteins pro-duced by ameloblasts in teeth work as a matrix to guide the growth direction of HA. Osteocalcin, *i.e.*, the most abundant non-collagenous protein of the bone's extracellular matrix, has been suggested to regulate the crystal growth of HA *via* specific adsorption on the *c* face. Specific macromolecules finely control the nucleation and the crystal growth of HA. Proteins and their related molecules could be utilized as regu-lators for use in biomaterial engineering.

Several peptides binding to a specific atomic arrangement were used to fabricate nanoscale materials.[3] Gungormus *et al.* reported the amino acid sequence of HA-attaching pep-tides that are identified by using phage display.[4] An artificial linear peptide (NPPTRQTKPKRVANTN) binding to the *c* face of HA was obtained using the mRNA display method.[5] The results of this study suggest that the amino acid sequence including Ala–Asn–Thr (ANT) is essential for binding specific-ity. The crystal growth of HA was found to be modulated by particular peptides.

Artificial calcium phosphate crystals with controlled sizes and shapes have been widely used in biomedical and dental applications.[6] Various morphologies of HA, such as fine parti-cles,[7] hexagonal rods,[8] and thin plates,[9] were synthesized by precipitation in a mixture of solutions containing calcium and phosphate ions[10–15] and transformation of various solid precursor crystals.[16–18] The next great challenge is the control of the orientation of HA nanocrystals mimicking the enamel structures. In the present work, we fabricated highly oriented columnar structures of HA similar to dental enamel through a controlled crystal growth method in a supersaturated solu-tion. Various approaches have been reported for the prepara-tion of oriented architectures mimicking natural bones.[19–21] Mesoscopically-ordered bone-mimetic nanocomposites were fabricated through mineralization of polymerized liquid crys-tals.[21] An organized structure of a fluorapatite (FA)–gelatin system was shown to resemble the biosystem in both bone and dentine.[22] A direct growth method to produce enamel-like prism structures of FA on metal plates was demonstrated using a hydrothermal technique.[23] The enamel-like HA bun-dle structures were obtained with monolayers of surfactants at the air–water interface.[24] Spatial organization of HA nano-rods on a functionalized substrate was achieved *via* crystal growth with gelatin as a structure-directing agent.[25] Despite these efforts, the oriented structure of HA bundles has not been sufficiently controlled in artificial systems. Therefore, the production of enamel-like columnar structures toward

a Department of Applied Chemistry, Faculty of Science and Technology, Keio University, 3-14-1 Hiyoshi, Kohoku-ku, Yokohama 223-8522, Japan. E-mail: hiroaki@applc.keio.ac.jp
b Department of Crystalline Materials Science, Graduate School of Engineering, Nagoya University, Furo-cho, Chikusa-ku, Nagoya 464-8603, Japan

biomedical and dental applications remains challenging in the field of materials chemistry.

Sheet-like HA crystals are commonly prepared in a simulated body fluid (SBF) containing inorganic ions nearly equal to those of human blood plasma.[9,26] Nanometric low-dimensional forms, such as sheets and needles elongated in the *c* axis, were produced with phosphate-surplus or calcium-deficient HA in an SBF-based solution at human body temperature.[27] The enamel-like columnar structures were fabricated on a crystalline substrate in the SBF-based system.[19] Epitaxial growth on the *c*-face HA substrates was successfully controlled by changing the conditions. However, highly controlled growth techniques are required to promote the formation of oriented HA nanocrystals at a specific site without the crystalline substrate.

In the current research, enamel-mimetic apatite films consisting of *c*-axis-oriented nanorods were fabricated by a two-step crystal growth method in an aqueous solution system that was based on an SBF. The nucleation of apatite crystals was initiated with the monolayer of a specific artificial peptide binding to the *c* face of HA. The formation of *c*-axis-oriented films with apatite microrods was promoted through geometric selection in the presence of fluoride ions. The subsequent growth with D-aspartic acid produced the enamel-like structure consisting of oriented nanorods on the basal microrods. The stepwise crystal growth controlled by the specific artificial peptide, fluoride ion, and aspartic acid could be utilized for fabrication of well-organized biomaterials that consist of oriented nanoscale HA nanocrystals.

Experimental

Formation of HA films on the peptide monolayer

An artificial linear peptide (NPPTRQTKPKRVANTN, Scheme 1) that binds to the *c* face of HA was used to promote the nucleation of HA. A stearoyl group was bound to the N-terminus of the peptide to form a molecular layer at the air–water interface. A Langmuir monolayer of the peptide was prepared in aqueous solution by spreading a 0.4 mg cm^{-3} solution of the peptide dissolved in a mixture of dimethyl sulfoxide and chloroform. Isotherms of the surface pressure and area of the peptide monolayer were obtained using a United System Integrators FSD-50 in pure water and in the mineralizing solution, *i.e.*, SBF at room temperature. A common SBF is the buffered mineralization solution containing the various ions of human blood plasma.[8] In the present study, we used an SBF-based solution (s-SBF$_{1.0}$) simplified by the removal of minor ions, such as Mg^{2+}, SO_4^{2-}, and HCO_3^-. s-SBF$_{1.0}$ was prepared by mixing HCl (Junsei Chemical), $CaCl_2 \cdot 2H_2O$ (Junsei Chemical), Na_2HPO_4 (Junsei Chemical), and NaCl (Kanto Chemical) with purified water. The concentrations of Ca^{2+}, HPO_4^{2-}, Na^+, and Cl^- were 2.5, 1.0, 141.0, and 165.0 mM, respectively. The pH was adjusted to a certain value between 6.4 and 7.2 by adding tris(hydroxymethyl)-aminomethane (Junsei Chemical) to control the growth conditions of HA crystals. We also increased the ion
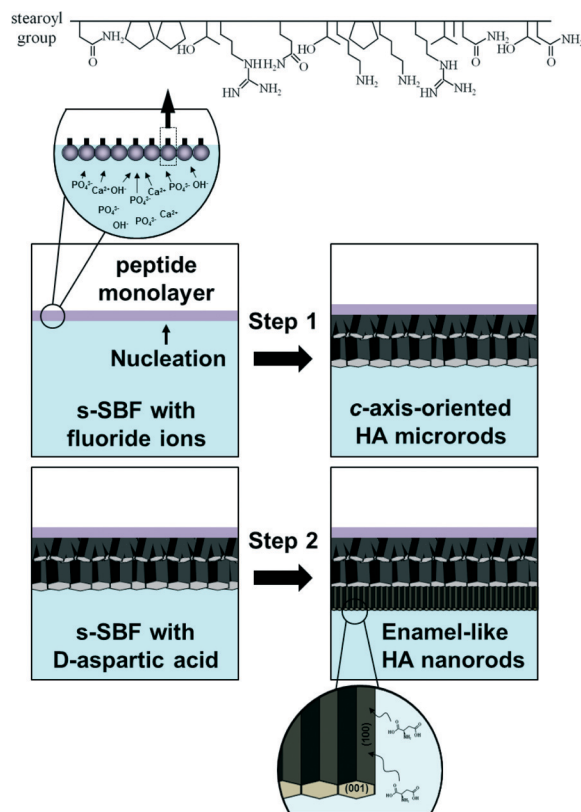
Scheme 1 Schematic representation of the *c*-face-binding peptide and the fabrication process of enamel-like apatite nanorods using the peptide monolayer in s-SBF$_x$. The *c*-axis-oriented microrods are grown under the peptide monolayer with fluoride ions (Step 1). The enamel-like nanorod array is formed under the microrods with D-aspartic acid (Step 2).

concentrations in the supersaturated solutions to regulate the growth rate (s-SBF$_x$, $X = 1.0$–2.0). The ion concentrations in s-SBF$_x$ were X times higher than those in s-SBF$_{1.0}$. The molecular layer of the peptide was then prepared in s-SBF$_x$. As a control experiment, stearic acid was spread at the air–water interface instead of the peptide. The solution was kept at 38 °C for a certain period. The resultant products were washed with pure water and air-dried at room temperature for 24 h.

Effects of fluoride ion

Sodium fluoride (Kanto Chemical) was added to s-SBF$_x$ ($X = 1.0$–2.0) to study the effect of the fluoride ion on the crystal growth of HA. The concentration of the fluoride ion was set at a specific value in the range from 0.53 to 1.1 mM, and the pH was adjusted to 6.8. The solution was kept at 38 °C for 24–120 h. The preparation conditions were adjusted according to a previous study.[28]

Preparation of enamel-like oriented nanorods

As shown in Scheme 1, we prepared enamel-like oriented HA nanorods on the basal layer consisting of *c*-axis-oriented HA microrods produced with fluoride ions. The basal layer of HA

microrods was obtained under the peptide monolayer in s-SBF$_{1.2}$ containing fluoride ions at 38 °C for 120 h (Step 1). Addition of D-aspartic acid (Wako Pure Chemical) to s-SBF$_x$ was effective for miniaturization of HA rods grown in the solutions. Epitaxial growth was achieved on the basal layer at 38 °C in s-SBF$_{1.0}$ (pH 6.4) that contained 8.3 mM D-aspartic acid (Step 2).

Characterisation

The structures of the products were characterized using a field-emission scanning electron microscope (FESEM, Hitachi S-4700) and an environmental scanning electron microscope (ESEM, FEI Inspect S50) equipped with an energy-dispersive X-ray spectrometer (EDX, Bruker Quantax). The X-ray diffraction (XRD) patterns were recorded using a Bruker D8 Discover. The products were analyzed using the KBr method by Fourier transform infrared adsorption (FT-IR, Jasco FT-IR 4000).

Results and discussion

Formation of peptide monolayers

Fig. 1 shows the surface pressure–area (π–A) isotherms of the peptide having a stearoyl group in pure water and s-SBF$_{1.6}$. The π value increased linearly with decreasing A, indicating the formation of a stable monolayer of the peptide. From the π–A isotherms, the occupied area of the peptide molecule was estimated to be 42 and 38 nm^2 in water and s-SBF$_{1.6}$, respectively. The difference in the isotherms is indicative of the interactions of the peptide monolayers with various ions.

Formation of self-standing HA films under the peptide monolayer

According to the π–A isotherms, we obtained peptide monolayers in s-SBF by adjusting the molecular concentration at the air–water interface. As shown in Fig. 2, white products were observed with the peptide monolayer at the air–water interface in s-SBF$_{1.0}$ at pH 7.2, s-SBF$_{1.6}$ at pH 6.8–7.2, and s-SBF$_{2.0}$ at pH 6.0–7.2 for 24 h. In the absence of the peptide monolayer or the presence of a monolayer of stearic acid, no products were observed in the system. On the other hand, a
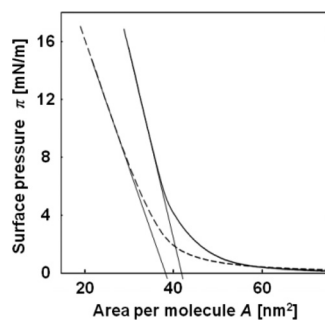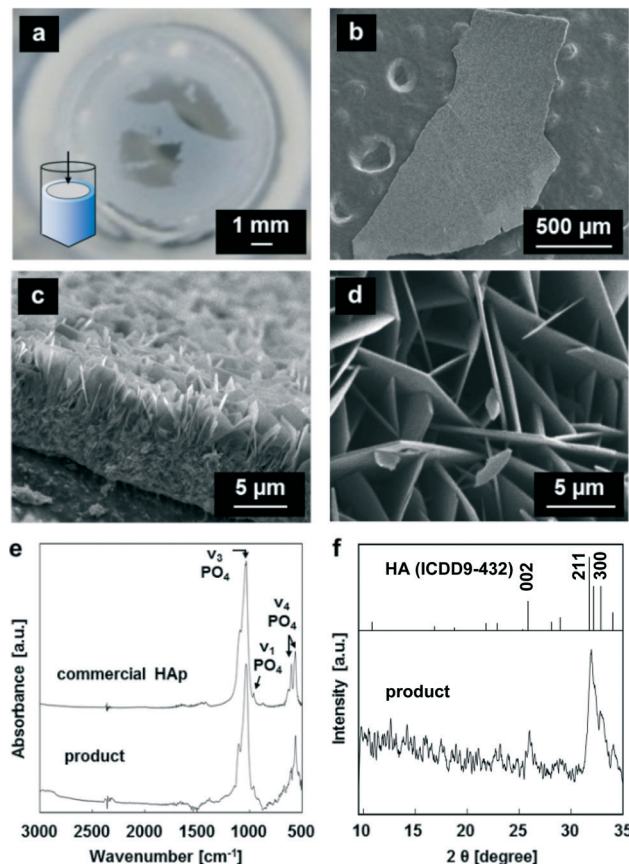

Fig. 2 Typical photograph (a) and SEM images (b, c) of the products under the peptide monolayer at the air–water interface of s-SBF$_{2.0}$ at pH 7.2. Typical SEM image (d), FT-IR (e), and XRD pattern (f) of the products under the peptide monolayer at the air–water interface of s-SBF$_{1.6}$ at pH 6.8.

self-standing white film was formed with the peptide monolayer (Fig. 2a). The self-standing films $ca.$ 20 μm in thickness were composed of nanoplates 100–500 nm thick that were grown from the monolayer (Fig. 2d). According to the specific diffraction signals in the XRD patterns and the absorption bands at 565 and 604, 962, and 1020 cm^{-1} assignable to ν_4, ν_1, and ν_3 vibration modes of PO$_4$, respectively, in the FT-IR spectra, the products were identified as HA (Fig. 2e and f). These results indicate that the peptide monolayer induced the formation of HA through heterogeneous nucleation in the supersaturated solution. However, the specific crystallographic orientation was not observed for the produced films consisting of HA plates.

Formation of c-axis-oriented films with fluoride ions

When 0.53 mM fluoride ions was added to s-SBF$_{1.6}$, a self-standing film consisting of nanorods $ca.$ 250 nm in diameter was produced at the interface (Fig. 3a and b). The thickness of the film was found to be ~15 μm after the oriented growth under the peptide monolayer for 24 h. The intense 002 diffraction peak was clearly observed in the XRD pattern of the film (Fig. 3f). Because the 002 signal was greater than the 300
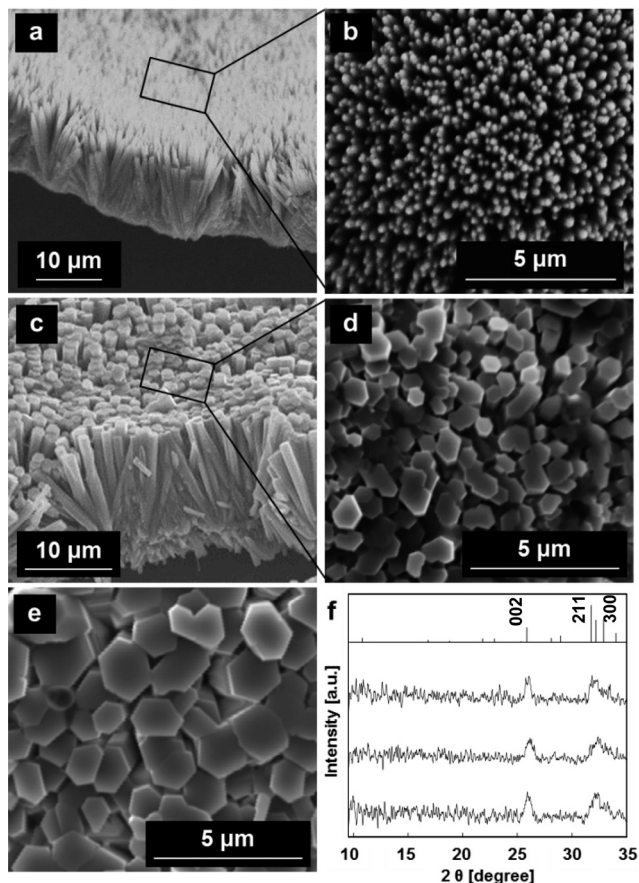

Fig. 1 Surface pressure and area (π–A) isotherms of the peptide in pure water (solid line) and s-SBF$_{1.6}$ at pH 6.8 (broken line).

Fig. 3 SEM images (a–e) and XRD patterns (f) of the films grown in s-SBF$_{1.6}$ with fluoride ions at pH 6.8. The products were grown in s-SBF$_{1.6}$ with [F$^-$] = 0.53 mM (a, b, i), with [F$^-$] = 1.1 mM (c, d, ii), and in s-SBF$_{1.2}$ with [F$^-$] = 1.1 mM (e, iii).

reflection, the nanorods in the films were preferentially oriented with their c-axes perpendicular to the substrate. The radial growth of the nanorods from a nucleation point was observed in the cross-sectional image. Thus, the oriented growth of the nanorods was achieved through geometric selection. Because we confirmed the presence of fluoride ions in the film by EDX, we can infer that the hexagonal rods were produced through substitution of hydroxy groups with fluoride ions. Consequently, we obtained the FA or fluorine-doped HA film consisting of c-axis-oriented nanorods that were preferentially aligned on the surface.

The rod diameter increased to ~1 μm with the formation of hexagonal facets by increasing the fluoride concentration up to 1.1 mM (Fig. 3c and d). According to the enhanced 002 signal, the degree of the c-axis orientation was improved by increasing the fluoride ion concentration. Furthermore, the width of the hexagonal rods gradually increased to ~2 μm for 120 h (Fig. 3e). These oriented architectures are similar to the rod array of the enamel layer. However, the films were relatively porous with a low concentration of fluoride ions (Fig. 3b), and the rods were very thick with a high concentration of fluoride ions (Fig. 3d) as compared with the biogenic enamel structure.

Formation of enamel-like architectures through the subsequent growth with D-aspartic acid

As shown in Scheme 1, we fabricated enamel-like architectures consisting of c-axis-oriented HA nanorods by subsequent growth on the basal microrods prepared with fluoride ions with the peptide monolayer (Fig. 4a and c). The array composed of hexagonal rods 1–2 μm in diameter was used as the basal layer (Step 1) (Fig. 3e). In a previous study, we reported that the selective attachment of DL-aspartic acid to Ca^{2+} on the a face decreases the diameter of the HA rods.[19] We confirmed that D-aspartic acid has the same effect as DL-aspartic acid. Thus, nanorod arrays would be produced in the presence of D-aspartic acid. In the progressive stage (Step 2), the nanorods ca. 100 nm in diameter were formed through epitaxial growth on the basal layer (Fig. 4b). The XRD profiles after the subsequent growth were not changed from the basal layer. Because D-aspartic acid was identified by characteristic absorption bands around 1200–1700 cm^{-1} in FT-IR spectra (Fig. 4d), the specific adsorption of D-aspartic acid on the a faces decreased the size of the nanorods. In consequence, the enamel-like oriented HA architectures were obtained under the peptide monolayer by a two-step controlled crystal growth method. When aspartic acid was added to the first step, the c-axis-oriented HA architectures were not produced at the interface due to the strong interaction of the organic molecule to the nucleation site. Thus, the subsequent growth on the basal layer prepared with fluoride ions is valid for the synthesis of nanometric-oriented architectures.

Conclusions

A two-step controlled crystal growth technique was developed to produce enamel-like oriented nanorods using a specific
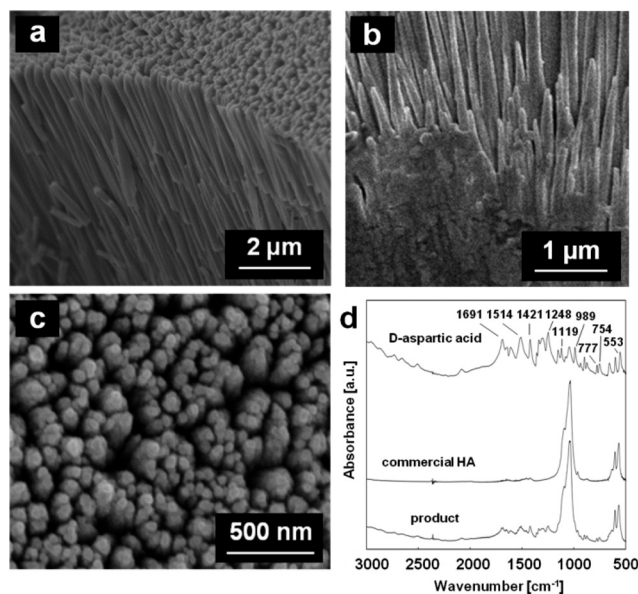

Fig. 4 SEM images: cross-sectional views (a, b), plane view (c) and FT-IR spectra (d) of the products on the basal layer of the oriented microrods grown in s-SBF$_{1.0}$ with D-aspartic acid for 120 h.

artificial peptide, fluoride ions, and D-aspartic acid. The monolayer of the peptide binding to the *c* face of HA was used as the nucleation site at the air–water interface. Self-standing films with *c*-axis-oriented microrods were formed through geometric selection under the monolayer in an aqueous solution system that was based on a simulated body fluid containing fluoride ions. The subsequent growth with aspartic acid produced the enamel-like structure consisting of oriented nanorods on the basal microrods. The controlled growth with the specific artificial peptide is applicable for fabricating well-organized biomaterials that consist of oriented nanoscale HA crystals.

Acknowledgements

Notes and references

1 L. Li, C. Mao, J. Wang, X. Xu, H. Pan, Y. Deng, X. Gu and R. Tang, *Adv. Mater.*, 2011, **23**, 4695.
2 T. Nakano, K. Kaibara, T. Ishimoto, Y. Tabata and Y. Umakoshi, *Bone*, 2012, **51**, 741.
3 Y. J. Lee, H. Yi, W. J. Kim, K. Kang, D. S. Yun, M. S. Strano, G. Ceder and A. M. Belcher, *Science*, 2009, **324**, 1051.
4 M. Gungormus, H. Fong, I. W. Kim, J. S. Evans, C. Tamerler and M. Sarikaya, *Biomacromolecules*, 2008, **9**, 966.
5 S. Ono, T. Tsuji, Y. Oaki and H. Imai, *RSC Adv.*, 2013, **3**, 1885.
6 K. Lin, C. Wu and J. Chang, *Acta Biomater.*, 2014, **10**, 4071.
7 D. Wang and F. Caruso, *Adv. Mater.*, 2001, **13**, 350.
8 H. Ito, Y. Oaki and H. Imai, *Cryst. Growth Des.*, 2003, **8**, 1055.
9 T. Kokubo and H. Takadama, *Biomaterials*, 2006, **27**, 2907.
10 I. S. Neira, F. Guitian, T. Taniguchi, T. Watanabe and M. Yoshimura, *J. Mater. Sci.*, 2008, **43**, 2171.
11 I. S. Neira, Y. V. Kolen'ko, O. I. Lebedev, G. V. Tendeloo, H. S. Gupta, F. Guitian and M. Yoshimura, *Cryst. Growth Des.*, 2009, **9**, 466.
12 K. Ioku, S. Yamauchi, H. Fujimori, S. Goto and M. Yoshimura, *Solid State Ionics*, 2002, **151**, 147.
13 M. J. Olszta, X. Cheng, S. S. Jee, R. Kumar, Y. Y. Kim, M. J. Kaufman, E. P. Douglas and L. B. Gower, *Mater. Sci. Eng., R*, 2007, **58**, 77.
14 S. Suzuki, M. Ohgaki, M. Ichiyanagi and M. Ozawa, *J. Mater. Sci. Lett.*, 1998, **17**, 381.
15 B. Viswanath and N. Ravishankar, *Biomaterials*, 2008, **29**, 4855.
16 W. E. Brown, *Nature*, 1962, **196**, 1048.
17 W. E. Brown, *Clin. Orthop. Relat. Res.*, 1966, **44**, 205.
18 M. D. Francis and N. C. Webb, *Calcif. Tissue Res.*, 1971, **6**, 335.
19 W. Wang, Y. Oaki, C. Ohtsuki, T. Nakano and H. Imai, *J. Asian Ceram. Soc.*, 2013, **1**, 143.
20 S. Hayakawa, Y. Li, K. Tsuru, A. Osaka, E. Fujii and K. Kawabata, *Acta Biomater.*, 2009, **5**, 2152.
21 W. He, A. K. Rajasekharan, A. R. Tehrani-Bagha and M. Andersson, *Adv. Mater.*, 2015, **27**, 2260.
22 P. Simon, D. Zahn, H. Litchte and R. Kniep, *Angew. Chem., Int. Ed.*, 2006, **45**, 1911.
23 H. Chen, Z. Tang, J. Liu, K. Sun, S. R. Chang, M. C. Peters, J. F. Mansfield, A. Czajka-Jakubowska and B. H. Clarkson, *Adv. Mater.*, 2006, **18**, 1846.
24 Y. Xu, G. Ma, X. Wang and M. Wang, *Cryst. Growth Des.*, 2012, **12**, 3362.
25 Y. Tseng, M. E. Birkbak and H. Birkedal, *Cryst. Growth Des.*, 2013, **13**, 4213.
26 T. Kokubo, S. Ito, T. Huang, T. Hayashi, S. Sakka, T. Kitsugi and T. Yamamuro, *J. Biomed. Mater. Res.*, 1990, **24**, 331.
27 T. Kobayashi, S. Ono, S. Hirakura, Y. Oaki and H. Imai, *CrystEngComm*, 2012, **14**, 1143.
28 Y. Fan, J. R. Nelson, J. R. Alvarez, J. Hagan, A. Berrier and X. Xu, *Acta Biomater.*, 2011, **7**, 2293.